

A Novel Downlink IM-NOMA Scheme

ABDULLATEEF ALMOHAMAD¹ (Member, IEEE), MAZEN O. HASNA¹ (Senior Member, IEEE),
SAUD ALTHUNIBAT² (Senior Member, IEEE), AND KHALID QARAQE³ (Senior Member, IEEE)

¹Department of Electrical Engineering, Qatar University, Doha, Qatar

²Department of Communications Engineering, Al-Hussein Bin Talal University, Ma'an 71111, Jordan

³Department of Electrical and Computer Engineering, Texas A&M University at Qatar, Doha, Qatar

CORRESPONDING AUTHOR: A. ALMOHAMAD (e-mail: abdullateef@ieee.org)

This work was supported in part by the Qatar National Research Fund under Grant NPRP12S-0225-190152

(a member of The Qatar Foundation), and in part by Qatar National Library.

ABSTRACT In the next generations of communication systems, resources' scarcity devolves to a more critical point as a consequence of the expected massive number of users to be served. Furthermore, the users' contradicting requirements on quality of service forces the network to behave in a dynamic way in terms of the multiple access orchestration and resource assignment between users. Hence, the linear relation between the number of served users and the required (orthogonal or semi-orthogonal) resources in the orthogonal multiple access (OMA) schemes is no longer sufficient. As promising candidates, Non-orthogonal multiple access (NOMA) schemes and index modulation (IM) techniques are emerging to satisfy the ever-increasing connectivity demands and spectral efficiency. In this article, a novel IM-based NOMA downlink scheme, termed as IM-NOMA, is proposed, where the base station (BS) selects a channel or more to serve each user based on the IM concept and the corresponding power level is allocated based on the NOMA concept. At the users' ends, maximum likelihood and successive interference cancellation (SIC) detection methods are considered and their error rate, outage probability and computational complexity are studied. Simulation results confirm the advantage of the proposed IM-NOMA scheme and that it can outperform the conventional NOMA system.

INDEX TERMS NOMA, index modulation, multiple access, OFDMA.

I. INTRODUCTION

THE SPECTRUM scarcity and the power resources limitations in addition to the expected large number of users are considered among the main challenges towards future communication systems. As the deployment of Internet of Things (IoT) nodes is being widely adopted, billions of connected users/nodes with different quality of service (QoS) requirements are expected to be served by future networks [1]. Moreover, fulfilling a wide range of contradicting QoS requirements limits the effectiveness of the current solutions. Hence, revolutionary and innovative techniques should be proposed and matured on the road to efficiently handle the connectivity demands [2].

Among the recent proposed physical layer techniques that demonstrate promising performance are Index Modulation (IM) [3] and Non-Orthogonal Multiple Access (NOMA). In IM, data blocks are conveyed between two communicating

nodes not only by conventional complex constellation points, but also via the index of the transmit entity (such as the transmit antenna, the operating frequency or the occupied time slot). As such, spectral efficiency is significantly improved and error performance is also shown to be enhanced. Recently, exploiting the appealing performance achieved by the IM techniques, it was employed in a broad spectrum of systems, such as orthogonal frequency division multiplexing (OFDM) [3]–[7], multiple-input multiple-output (MIMO) [8], [9], wireless sensor networks [10], cooperative and cognitive networks [11], [12] and on the signals' polarization [13].

NOMA has also been widely nominated as a spectral efficient multiple access scheme compared to traditional ones [14]. More specifically, in NOMA systems, multiple users can utilize the same channel simultaneously, which

significantly improves the spectral efficiency [15]. In power domain NOMA (PD-NOMA), the most popular variant of downlink NOMA schemes, different users are allocated different power levels according to their experienced channel conditions, in which less power is assigned to the user with good channel condition and vice versa. Hence, satisfying users' different QoS requirements can be done by adjusting the power allocation scheme [16]. Inter-user interference introduced by allowing multiple users to share the same channel can be handled and canceled by employing special detection techniques such as successive interference cancellation (SIC).

Adopting IM in the context of multiple access scenarios has been recently introduced in [17]–[19], where different variants of uplink multiple access schemes have been proposed and analyzed. However, those schemes show good performance only in the uplink scenario. Recently, two related schemes were proposed considering the case of two users [20], [21]. In both schemes, the near user applies OFDM by occupying all available subcarriers, while OFDM-IM [3] is applied by the far user. Moreover, [20] considers the downlink case while the scheme in [21] is proposed for the uplink scenarios. Thus, adopting PD-NOMA concept, power domain multiplexing is done for the users' signals. Detection computational complexity arises as an inherited drawback when adopting IM concept in any communications system. A log likelihood ratio (LLR)-based detection algorithm was proposed in [22], where it is shown that it achieves near optimal performance while maintaining a relatively low complexity as compared to ML detection. Another low complexity detection method was proposed in [23] based on the constellation rotation, and was shown to significantly reduce the SIC complexity for the case of two users. A similar IM-aided NOMA scheme was proposed in [24] for visible light communications (VLC), where users are clustered in pairs. For each pair, one user is served using conventional OFDM, and data of the other is conveyed using IM-based on-off keying concept. More recently, a combination of IM and uplink NOMA was studied in [25], [26], where both proposed schemes fit for the case of two users in the uplink direction. Furthermore, in [26] a cooperative NOMA is considered where one of the users plays the role of a relay to forward messages to the second user. Spatial modulation (SM) [27] was considered as a special case of IM, where the indices of the transmit antennas are used to convey the extra information to the receiver. In addition, few works have considered the integration between SM and NOMA [28], [29]. In [28], SM was applied in a MIMO system where a single antenna is activated per user, and power allocation scheme is applied to mitigate the inter-user interference. A similar scheme was proposed in [29] in which cooperative NOMA is assumed and the case of two users only is considered. It is worth mentioning here that all multi-user SM-based systems suffer from high cost and low power efficiency due to having high number of RF chains [30].

For instance, in downlink communications, the number of required RF chains should equal the number of served users. However, few works, [29], [31], [32], have proposed a modified SM-NOMA schemes, utilizing a single RF chain, to improve power efficiency and reduce hardware implementation complexity. Nevertheless, those schemes are applicable to the case of two users only, where the spatial bits are transmitted to a single user and the complex modulated symbols are transmitted to the other user. A more similar downlink IM-NOMA scheme has been proposed recently in [33]. However, it considers only the simplified case of two users in the system model and the derivation of the error performance under the SIC detection. Furthermore, the interference between users is neglected in the derivation which might give acceptable analytical results in the two users' case. For the general case, it is expected to result in a loose bound on the performance as the number of users increases. Moreover, the error performance under SIC detection is the only investigated metric in this work while investigating other metrics such as the outage probability and the diversity gain of such systems (as considered in this article) is important to give more insights of newly proposed schemes.

As seen in the above discussion, the related works assume special cases which limit the flexibility of the proposed scheme. Specifically, the case of only two users has been considered in [20], [21], [24]–[26], [29], [31]–[33] with a limited analytical performance analysis. In [20], [21], only one user applies IM-OFDM while the second user applies NOMA-OFDM. Only the uplink transmission scenario has been adopted in [17]–[19], [21]. Finally, in [36] and [39], a cooperative scenario is assumed where a user functions as a relay for the other user. Clearly, a system under these assumptions cannot be generalized, and will suffer from inflexibility especially when adopting more complicated cases such as multiple non-cooperative users, general power allocation method and/or different subcarrier activation ratio per user. In this article, leveraging the advantages of both the IM and NOMA schemes, and targeting the explained gap in the available literature, a new downlink multiple access scheme called index-modulation based NOMA (IM-NOMA) is proposed. The proposed scheme implies that the base station (BS) selects the subcarrier(s) over which the signal of a user is transmitted based on part of its data, employing the IM principle. Additionally, the BS divides the total transmit power among users following the NOMA principle, where the allocated power level for a user is inversely proportional to its channel conditions. Such a novel scheme can leverage the benefits of both IM and NOMA to present a flexible and enhanced downlink scheme in terms of the error performance and the number of served users. The contributions of this work can be summarized as follows:

- A novel IM-based NOMA scheme is proposed that leverage the power efficiency and flexibility of IM and the spectral efficiency of NOMA.

- The error performance of the proposed scheme is analyzed under two detection schemes, namely ML and SIC, considering Rayleigh fading channels.
- The computational complexity of the proposed scheme is studied and compared with that of PD-NOMA.
- The outage probability of the proposed scheme is derived in a closed-form formula for both detection schemes. In addition, the diversity gain is studied for the SIC detection case.
- Numerical simulations are provided to validate the analytical findings and to show the superiority of the proposed scheme over the conventional PD-NOMA and the recently proposed Hybrid IM-NOMA scheme.

The remainder of this article is organized as follows. Section II presents the proposed IM-NOMA system model. The error performance is investigated in Section III, followed by the outage probability and diversity gain analysis in Section IV, while the computational complexity is studied in Section V. Simulation results are explored in Section VI and conclusions are drawn in Section VII.

II. PROPOSED IM-NOMA SYSTEM MODEL

A downlink communication system is considered, where a single BS is serving N_T users over a total bandwidth of B_T . Similar to orthogonal frequency division multiple access (OFDMA) systems, the allocated bandwidth is divided into L_T orthogonal subcarriers each of B_c bandwidth. Now, a set of $N \leq N_T$ users is served by a chunk of L adjacent subcarriers. The users to chunks pairing can be done following the user pairing approaches in NOMA. In what follows, and without loss of generality, a single chunk is considered.

In the proposed IM-NOMA scheme, a total of B bits are delivered to each user during every transmission time. Specifically, the transmitted bits B for user n are split into two parts, the first of which consists of $\log_2 M$ bits and is mapped to a complex constellation symbol, c_n , drawn from a M -PSK modulation scheme. The second part which includes $\lfloor \log_2 \binom{L}{K} \rfloor$ bits, with $1 \leq K \leq L$, is used to select an active combination of subcarriers to carry the complex symbol c_n . Therefore, the signal to be transmitted to user n over subcarrier ℓ can be written as follows

$$s_{n\ell} = \begin{cases} c_n, & \text{if } \ell \in \hat{\ell}_n \\ 0, & \text{if } \ell \notin \hat{\ell}_n \end{cases} \quad (1)$$

where $\hat{\ell}_n$ represents the set of indexes of active subcarriers for the n^{th} user. Thus, the same process is followed for each user to select the complex symbol and the active subcarriers to carry it.

Next, similar to the classical PD-NOMA systems, signals to be sent to different users are multiplexed in power domain over all subcarriers and transmitted simultaneously. In specific, a power level is assigned to user n according to its distance from the BS, where a higher power level is allocated to farther users in order to compensate for the path

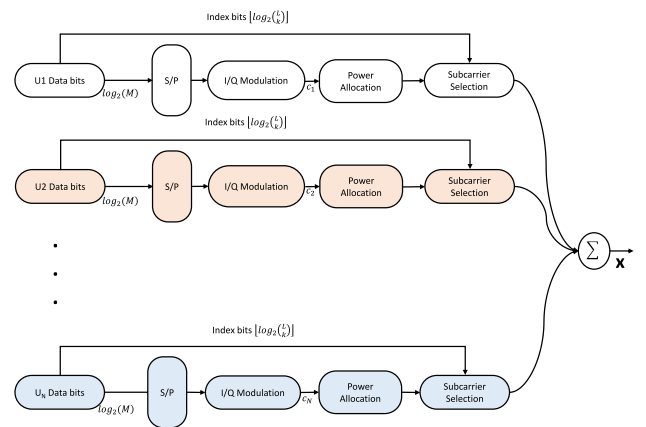


FIGURE 1. Downlink IM-NOMA System Model.

loss effect. The power of the signal to user n is scaled by the coefficient ρ_n , which is computed as follows [34]¹

$$\rho_n = \frac{d_n^2}{\sum_{i=1}^N d_i^2} \quad (2)$$

where d_n denotes the distance between user n and the BS. It is worth noting that the objective of this article is to propose an efficient and flexible scheme, hence a simple power allocation method is adopted. Further studies can be done to investigate the optimal power allocation and user pairing options. Moreover, the pairwise error probability (PEP) derivation in Section III is independent of the power allocation in (2), and hence it holds for other power allocation methods. Thus, the superimposed transmitted signal x_ℓ over subcarrier ℓ can be expressed as

$$x_\ell = \sum_{n=1}^N \sqrt{\rho_n} s_{n\ell}. \quad (3)$$

The received signal at user n over subcarrier ℓ is written as

$$y_{n\ell} = \sqrt{P_{r,n}} h_{n\ell} x_\ell + w_{n\ell}, \quad (4)$$

where $P_{r,n} = P_t d_n^{-\eta}$ represents the received power at user n , P_t is the total transmitted power, η is the path loss exponent, $h_{n\ell}$ denotes the experienced channel by user n over subcarrier ℓ , and $w_{n\ell} \sim \mathcal{CN}(0, \sigma_n^2)$ represents the additive white Gaussian noise at user n over subcarrier ℓ . We assume that the channel coefficients between the different users and the BS are independent and identically distributed (i.i.d) Rayleigh fading channels.

In what follows, ML and SIC detection methods are considered to decode the transmitted bits for each user.

1. Power allocation can be done following different approaches as per the amount of knowledge about the CSI. For instance, it can be a function of the users' average channel gains (distances) [35] or based on the channel CSI [36], [37].

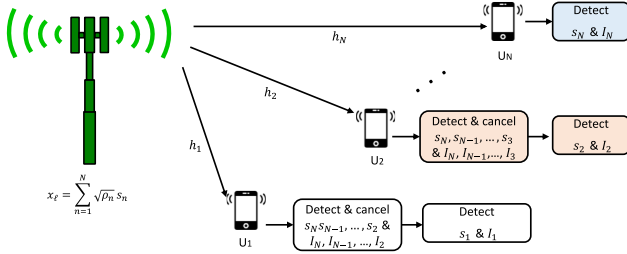


FIGURE 2. IM NOMA with SIC Detection Block Diagram.

A. MAXIMUM LIKELIHOOD DETECTION (ML)

In this detection technique, as a multi-user detection, the transmitted signals of all users are jointly decoded at each user. Define the vectors $\mathbf{y}_n = [y_{n1}, y_{n2}, \dots, y_{nL}]$ and $\mathbf{x}_n = [x_1, x_2, \dots, x_L]$ respectively representing the received and transmitted signals over all subcarriers in the considered chunk at user n . Accordingly, the matrix form of (4) is written as

$$\mathbf{y}_n = \sqrt{P_{r,n}} \mathbf{h}_n \odot \mathbf{x} + \mathbf{w}_n, \quad (5)$$

where $\mathbf{h}_n = [h_{n1}, h_{n2}, \dots, h_{nL}]^T$, \odot is the element-wise product, and $\mathbf{w}_n = [w_{n1}, w_{n2}, \dots, w_{nL}]^T$.

The signals of all users are detected at once at user n by applying ML detection as follows

$$\hat{\mathbf{x}} = \arg \min_{\mathbf{x}^{(i)} \in \mathcal{X}} \|\mathbf{y}_n - \sqrt{P_{r,n}} \mathbf{h}_n \odot \mathbf{x}^{(i)}\|^2, \quad (6)$$

where $\|\cdot\|^2$ is the squared Euclidean norm, and the set of all candidate combinations of transmission vectors is denoted as \mathcal{X} . It is worth noting that the set \mathcal{X} contains 2^{NB} different transmitted vectors candidates that need to be checked in ML detection before making a detection decision. Hence, the favorable optimal performance of ML detection is obtained with the cost of high computational complexity which might not be affordable, especially at large values of N , L and/or M .

B. SUCCESSIVE INTERFERENCE CANCELLATION DETECTION (SIC)

SIC detection is known to be a good alternative to reduce the high computational complexity of the ML technique at the cost of a slight performance degradation. In SIC, each user should decode and cancel the signals of the other users that are farther than him. Specifically, user n will first detect the signal vector of user N , \mathbf{s}_N , (the farthest user from the BS) assuming all other signals as noise. The detected signal vector \mathbf{s}_N will then be subtracted from the received signal vector. This same procedure is repeated till user n extracts its own signal. Note that the first user, i.e., the closest user, needs to cancel the signals of all other users, while user N , the farthest user, does not cancel any signal and directly detects its signal while treating all other users' signals as noise.

Mathematically, user n will detect its own signal vector as follows

$$\hat{\mathbf{s}}_n = \arg \min_{\mathbf{s}_n^{(i)} \in \mathcal{S}_n} \|\mathbf{y}'_n - \sqrt{P_{r,n}} \rho_n \mathbf{h}_n \odot \mathbf{s}_n^{(i)}\|^2, \quad (7)$$

where \mathcal{S} is the set of all possible candidate transmission vectors to a user, and \mathbf{y}'_n is the received signal after cancelling the farther users' signals, and is defined as

$$\mathbf{y}'_n = \mathbf{y}_n - \sqrt{P_{r,n}} \mathbf{h}_n \odot \left(\sum_{i=n+1}^N \sqrt{\rho_i} \hat{\mathbf{s}}_i \right). \quad (8)$$

III. ERROR PERFORMANCE ANALYSIS

Considering both detection techniques, ML and SIC, the average pairwise error probability (PEP) is derived in this section, where a closed form expression is derived for the ML case while an approximation is provided for the SIC counterpart. Then, the bit error rate's (BER) upper bound is obtained by employing the union bounding technique.

A. ML DETECTION ERROR PERFORMANCE

As per the union bounding method, the upper bound on the BER at user n is expressed in terms of the PEP as follows

$$\text{BER}_n = \frac{1}{2^{NB}} \sum_{i=1}^{2^{NB}} \sum_{j=1}^{2^{NB}} \tau_{ij,n} \text{PEP}_{ij} \quad (9)$$

with $\tau_{ij,n}$ representing the distance in terms of the number of different bits between the pair (i, j) under consideration, and PEP_{ij} is the PEP, which simply measures the likelihood of erroneously detecting the vector $\mathbf{x}^{(i)}$ while the transmitted vector is actually $\mathbf{x}^{(j)}$. Hence, incorporating (6), the PEP is rewritten as follows

$$\text{PEP}_{i,j} = \Pr \left\{ \|\mathbf{y}_n - \sqrt{P_{r,n}} \mathbf{h}_n \odot \mathbf{x}^{(i)}\|^2 > \|\mathbf{y}_n - \sqrt{P_{r,n}} \mathbf{h}_n \odot \mathbf{x}^{(j)}\|^2 \right\}. \quad (10)$$

Now, since the vector $\mathbf{x}^{(j)}$ was actually transmitted and by substituting (5), (10) can be simplified to be

$$\text{PEP}_{i,j} = \Pr \left\{ \|\mathbf{w}_n\|^2 > \|\sqrt{P_{r,n}} \mathbf{h}_n \odot \Delta_{ji} + \mathbf{w}_n\|^2 \right\}, \quad (11)$$

where $\Delta_{ji} = \mathbf{x}^{(j)} - \mathbf{x}^{(i)}$. Next, the conditional PEP can be written in terms of the Q function, for a given channel instance, as follows

$$\text{PEP}_{i,j|\mathbf{h}_n} = Q \left(\sqrt{\frac{\psi_{ji,n}}{2\sigma_n^2}} \right), \quad (12)$$

where $\psi_{ji,n} = \|\sqrt{P_{r,n}} \mathbf{h}_n \odot \Delta_{ji}\|^2 = p_{r,n} \sum_{\ell=1}^L |h_{n\ell} \delta_{\ell}|^2$, and δ_{ℓ} is the ℓ^{th} element in Δ_{ji} . Given that $\mathbf{h}_{n\ell} \sim \mathcal{CN}(0, 1)$, ψ_{ji} is a sum of L exponential random variables (RVs), where the mean of the ℓ^{th} RV is $\mu_{\ell} = p_{r,n} |\delta_{\ell}|^2$. Actually, there are $K \leq L$ RVs having nonzero means. Furthermore, there are R out of K RVs having unique means $\mu_1, \mu_2, \dots, \mu_R$.

Let us denote the number of RVs with the mean μ_i as r_i . Therefore, the PDF of $\psi_{ji,n}$ is given [38, eq. 9] as follows

$$f_{\psi_{ji,n}}(\varphi) = \sum_{q=1}^R \lambda_q^{r_q} e^{-\lambda_q \varphi} \sum_{\omega=1}^{r_q} A_{q,\omega} \frac{(-1)^{r_q-\omega}}{(\omega-1)!} \varphi^{\omega-1}, \quad (13)$$

where $A_{q,\omega} = \sum_{m_1+\dots+m_R=r_q-\omega} \prod_{\substack{t=1 \\ t \neq q}}^R \binom{r_t+m_t-1}{m_t} \frac{\lambda_t^{r_t}}{(\lambda_t-\lambda_q)^{r_t+m_t}}$ and

$$\lambda_\ell = \frac{1}{\mu_\ell}.$$

Then, by integrating (12) over the PDF given in (13) and following the same steps in [17] we get

$$\begin{aligned} \text{PEP}_{i,j} &= \sum_{q=1}^R \lambda_q^{r_q} \sum_{\omega=1}^{r_q} A_{q,\omega} (-1)^{r_q-\omega} \left(\frac{\chi_q}{\lambda_q} \right) \\ &\times \sum_{p=0}^{\omega-1} \binom{\omega-1+p}{p} (1-\chi_q)^p, \end{aligned} \quad (14)$$

where $\chi_q = \frac{1}{2} \left(1 - \frac{1}{\sqrt{1+4\sigma^2 \lambda_q}} \right)$. A more detailed derivation can be found in [39].

B. SIC DETECTION ERROR PERFORMANCE

Unlike the case in ML detection, in SIC each user retrieves its own data only after cancelling the interfering signals. Therefore, considering user n , $\text{PEP}_{ij,n}$ can be expressed as

$$\begin{aligned} \text{PEP}_{ij,n} &= \Pr \left\{ \left\| \mathbf{y}'_n - \sqrt{P_{r,n} \rho_n} \mathbf{h}_n \odot \mathbf{s}_n^{(i)} \right\|^2 \right. \\ &\quad \left. > \left\| \mathbf{y}'_n - \sqrt{P_{r,n} \rho_n} \mathbf{h}_n \odot \mathbf{s}_n^{(j)} \right\|^2 \right\} \end{aligned} \quad (15)$$

Eq. (15) can be formulated in terms of the Q function after some mathematical manipulations to yield

$$\text{PEP}_{ij,n|\mathbf{h}_n} = Q \left(\sqrt{\frac{P_{r,n} (\|\mathbf{g}_n\|^2 - \mathbf{g}_n^* \mathbf{t}_n)^2}{2 \|\mathbf{g}_n\|^2 \sigma^2}} \right) \quad (16)$$

where $\mathbf{g}_n = \mathbf{h}_n \odot \mathbf{b}_n$, $\mathbf{t}_n = \mathbf{h}_n \odot \mathbf{r}_n$, $\mathbf{b}_n = \mathbf{s}_n^{(i)} - \mathbf{s}_n^{(j)}$, $\mathbf{r}_n = \sum_{k=n+1}^N \sqrt{\rho_k} \mathbf{e}_k + \sum_{k=1}^{n-1} \sqrt{\rho_k} \mathbf{s}_k^{(i)}$, and $\mathbf{e}_k = \mathbf{s}_k^{(i)} - \mathbf{s}_k^{(j)}$. Such an equation cannot be mathematically tackled due to including rational correlated random variables that cannot be reduced. However, an approximation can be made for user N (the worst channel). As the user N has the highest power coefficient, we can assume that the values of other power coefficients are neglected. As such, $\mathbf{r}_n \approx \mathbf{0}$, and hence, $\mathbf{t}_n \approx \mathbf{0}$. Accordingly, (16) can be approximated for user N to yield

$$\text{PEP}_{ij,N|\mathbf{h}_n} \approx Q \left(\sqrt{\frac{P_{r,N} \|\mathbf{g}_N\|^2}{2\sigma^2}} \right) = Q \left(\sqrt{\frac{\psi'_{ij,N}}{2\sigma^2}} \right) \quad (17)$$

which can be solved using the same procedure in (12)-(14) to yield the same formula in (14) with replacing λ_q by $\lambda'_q = \frac{1}{\mu'_q}$, where $\mu'_\ell = P_{r,N} |\delta'_\ell|^2$ and δ'_ℓ is the ℓ^{th} element in \mathbf{b}_N .

IV. OUTAGE PROBABILITY AND DIVERSITY GAIN ANALYSIS

In what follows, outage probability expressions and the asymptotic diversity gain are derived for both detection techniques.

A. ML OUTAGE PROBABILITY

Considering the received signal at user n as in (4), the received instantaneous SINR can be expressed as follows

$$\text{SINR}_n = \frac{\|\sqrt{P_{r,n}} \mathbf{h}_n \odot \mathbf{x}\|^2}{\sigma_n^2}. \quad (18)$$

The outage probability at user n , denoted by $P_{o,n}$, can be written as

$$P_{o,n} = \Pr\{\text{SINR}_n < \gamma_{\text{th}}\}, \quad (19)$$

where γ_{th} denotes a given SINR threshold. Then, the outage probability $P_{o,n}$, using (18), can be written as follows

$$P_{o,n} = \Pr \left\{ \|\sqrt{P_{r,n}} \mathbf{h}_n \odot \mathbf{x}\|^2 < \gamma_{\text{th}} \sigma_n^2 \right\}, \quad (20)$$

which can be simplified, after expanding the norm and rearranging, to yield

$$P_{o,n} = \Pr \left\{ \sum_{\ell=1}^L |h_{n\ell}|^2 (\rho_n |s_{n\ell}|^2) < \frac{\gamma_{\text{th}} \sigma_n^2}{P_{r,n}} \right\}. \quad (21)$$

Consequently, the outage probability is the cumulative distribution function (CDF) of (13) evaluated at $\frac{\gamma_{\text{th}} \sigma_n^2}{P_{r,n}}$, which can be derived using [40, eq. 3.381.1] to yield

$$P_{o,n} = \sum_{q=1}^R \lambda_q^{r_q} \sum_{\omega=1}^{r_q} A_{q,\omega} \frac{(-1)^{r_q-\omega}}{(\omega-1)!} \left(\frac{1}{\lambda_q} \right)^\omega \gamma \left(\omega, \lambda_q \frac{\gamma_{\text{th}} \sigma_n^2}{P_{r,n}} \right), \quad (22)$$

where $\lambda_\ell = \frac{1}{\rho_n |s_{n\ell}|^2}$ and $\gamma(\cdot, \cdot)$ is the lower incomplete Gamma function.

B. SIC OUTAGE PROBABILITY

Unlike the ML detection method, which detects the data for all users at once, in SIC detection a user starts by cancelling the farther users' signals before detecting its own signal. Moreover, in IM-NOMA, and unlike PD-NOMA, not all users' signals are overlapping over all subcarriers but the inter-user interference happens based on the activation done by different users. The SINR in this case can be written as follows

$$\begin{aligned} \text{SINR}_n &= \frac{\sum_{\ell=1}^K |\sqrt{P_{r,n} \rho_n} h_{n\ell}|^2}{\sigma_n^2 + \sum_{m=1}^{n-1} P_{\text{col}}(m+1) \sum_{\ell=1}^K |\sqrt{P_{r,n}} h_{n\ell}|^2 \sum_{k=1}^m \sqrt{\rho_k}^2} \end{aligned} \quad (23)$$

where the summation in the denominator is done over the nearer users' signals that can not be cancelled at user n . $P_{\text{col}}(m)$ represents the probability of collision at a specific

subcarrier, i.e., the probability of the event of $m > 1$ users activate the same subcarrier, assuming the data source is uniformly random, and it is given as [17]

$$P_{\text{col}}(m) = \binom{N}{m} \left(\frac{1}{L}\right)^m \left(1 - \frac{1}{L}\right)^{N-m}. \quad (24)$$

The outage probability at user n is written in (25) on bottom of the page, which can be simplified after simple manipulations to

$$P_{o,n} = \Pr. \left\{ \sum_{\ell=1}^K |h_{n\ell}|^2 \leq \beta_{\text{th},n} \right\} \quad (26)$$

where $\beta_{\text{th},n} = \frac{\sigma_n^2 \gamma_{\text{th}}}{P_{r,n}(\rho_n - \gamma_{\text{th}} \sum_{m=1}^{n-1} P_{\text{col}}(m+1) (\sum_{k=1}^m \sqrt{\rho_k})^2)}$, and $\sum_{\ell=1}^K |h_{n\ell}|^2$ follows a Gamma distribution. Then

$$P_{o,n} = \frac{\gamma(K, \beta_{\text{th},n})}{\Gamma(K)}, \quad (27)$$

where $\gamma(\cdot, \cdot)$ is the lower incomplete Gamma function and $\Gamma(\cdot)$ is the Gamma function.

C. DIVERSITY GAIN

The diversity gain is the negative slope of the outage probability curve versus the SINR at asymptotically high SINR values in a log-log scale plot, which is written as

$$d_n = \lim_{\text{SINR} \rightarrow \infty} - \frac{\log(P_{o,n})}{\log(\text{SINR}_n)}. \quad (28)$$

From (27), noting that when $\text{SINR}_n \rightarrow \infty$ the term $\beta_{\text{th},n} \rightarrow 0$, and since the expansion of $\gamma(a, x)$ near 0 is $\gamma(a, x) \approx \frac{x^a}{a}$ [41], we get

$$d_n = \lim_{\text{SINR} \rightarrow \infty} - \frac{\log\left(\frac{\text{SINR}_n^{-K}}{K}\right)}{\log(\text{SINR}_n)} = K. \quad (29)$$

V. COMPLEXITY ANALYSIS

The computational complexity is usually expressed in terms of the number of real multiplications necessary for detection. In what follows, we calculate the computational complexity for both detection methods.

A. ML COMPUTATIONAL COMPLEXITY

As per the detection rule in (6), $6L$ real multiplications are required to perform $\sqrt{P_{r,n}} \mathbf{x}^{(i)} \odot \mathbf{h}_n$, while $2L$ multiplications are required to calculate the norm of the vector. Therefore, $8L$ multiplications are required to check a single candidate transmitted vector. Thus, since the set of all candidate transmission vectors contains a total of 2^{NB} vectors, the computational complexity at any user in IM-NOMA system applying ML detection is written as follows

$$CC_{ML} = 8L 2^{NB}. \quad (30)$$

B. SIC COMPUTATIONAL COMPLEXITY

The computational complexity induced by SIC detection at a user depends mainly on the number of the SIC iterations performed which, in turn, depends on the order of the corresponding user with respect to the others. Based on (7), each iteration requires $8L 2^B$ real multiplications. Consequently, the computational complexity in terms of the number of required real multiplications for the IM-NOMA scheme based on SIC detection technique for user n can be written as:

$$CC_{SIC,n} = 8L 2^B (N - n + 1), \quad (31)$$

where the coefficient $(N - n + 1)$ expresses the number of detection iterations performed at user n .

It is worth highlighting here that SIC provides a significant reduction in the computational complexity as compared to ML detection. Using (30) and (31), the percentage of complexity reduction due to employing SIC instead of ML at user n , denoted by $CCR_n\%$, can be expressed as follows

$$CCR_n\% = \left(1 - 2^{B(1-N)}(N - n + 1)\right) \times 100\% \quad (32)$$

where the maximum reduction percentage is achieved at user N , while the minimum reduction percentage occurs at the closest user (i.e., $n = 1$).

VI. NUMERICAL AND SIMULATION RESULTS

Simulation results are presented in this section to validate the analytical formulas and to compare the proposed scheme with the classical PD-NOMA, hybrid IM-NOMA [20] and SM-NOMA [28] schemes. Users are distributed such that the distance of user n from the BS is given as $d_n = \alpha d_{n-1}$, where $d_1 = 100\text{m}$ and $\alpha = 5$ is a distance multiplier. The path loss exponent is assumed as $\eta = 2.9$ and the noise power is set to $\sigma_n^2 = 10^{-10}$ Watts/Hz.

In Fig. 3, we fix the total transmit power at $P_T = 25$ dBm and plot the BER versus the power allocation coefficient of the near user, i.e., ρ_1 . We then sweep over the power coefficient ρ_1 between 0 and 1 with step of 0.01, while the remaining power is allocated to the far user, i.e., $\rho_2 = 1 - \rho_1$. From this figure, we find that the optimal power coefficients, that yield the minimum average BER are $\rho_1 = 0.04$ and $\rho_2 = 0.96$ for the near and far users, respectively. On the other hand, using our adopted power allocation method, in (2), the corresponding power coefficients are $\rho_1 = 0.0385$ and $\rho_2 = 0.9615$, which are close to the optimal ones. In fact, our power allocation method is designed based on intuition, with the distance squared in the numerator which, partially, cancels the effect of the path loss, and thus it maximizes the received SNR at both users. In the denominator, the

$$P_{o,n} = \Pr. \left\{ \frac{\sum_{\ell=1}^K |\sqrt{P_{r,n}} h_{n\ell}|^2}{\sigma_n^2 + \sum_{m=1}^{n-1} P_{\text{col}}(m+1) \sum_{\ell=1}^K |\sqrt{P_{r,n}} h_{n\ell}| \sum_{k=1}^m \sqrt{\rho_k}|^2} \leq \gamma_{\text{th}} \right\} \quad (25)$$

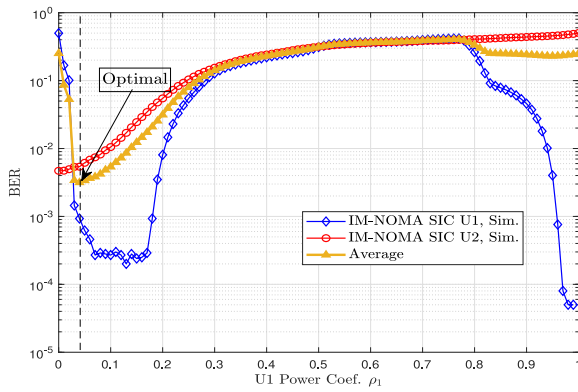


FIGURE 3. The BER performance of IM-NOMA versus the power coefficient of the near user with $N = M = L = 2$, $K = 1$ at a transmit power of $P_t = 25$ dBm.

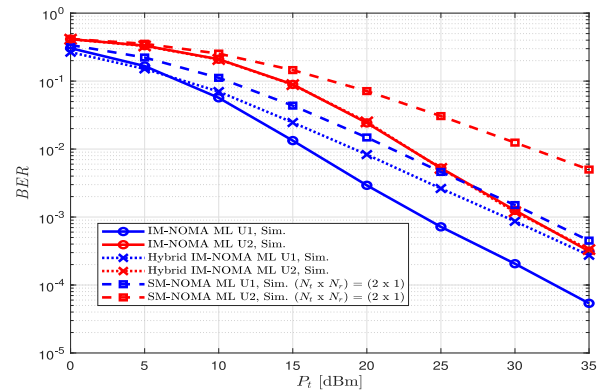


FIGURE 5. The average BER versus P_t at $N = L = M = 2$ for IM-NOMA ($K = 1$), hybrid IM-NOMA and SM-NOMA [28] with $N_t = 2$, $N_r = 1$.

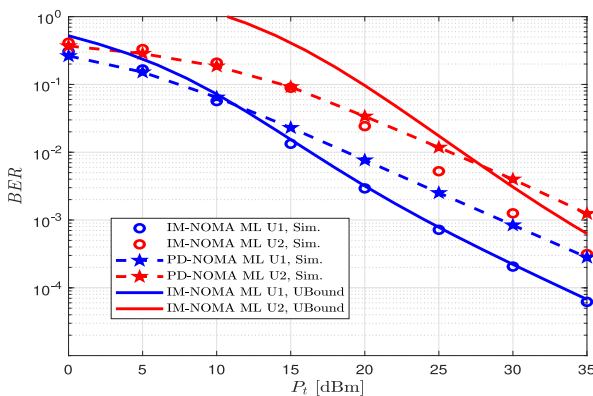


FIGURE 4. The average BER versus P_t at $N = L = M = 2$ for IM-NOMA ($K = 1$) and NOMA schemes.

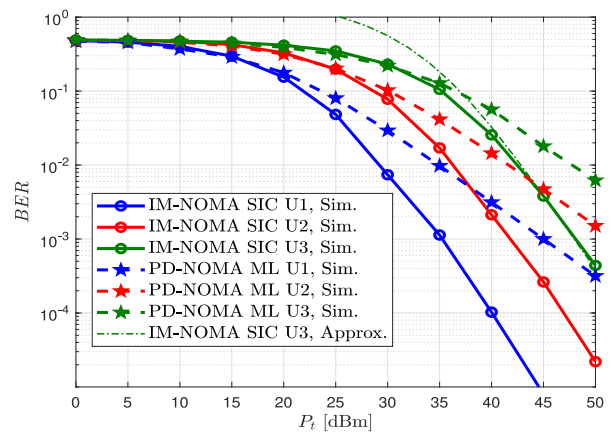


FIGURE 6. The average BER versus P_t at $N = L = 3$ and $M = 4, 2$ for IM-NOMA ($K = 1, 2$) and PD-NOMA schemes, respectively.

sum of all squared distances is used to normalize the power coefficients.

Fig. 4 plots the average BER of IM-NOMA and PD-NOMA schemes versus P_t considering $N = 2$ users, activating $K = 1$ subcarrier out of $L = 2$ available subcarriers and applying BPSK modulation, which sets the per user spectral efficiency at 2 bpcu. Comparing IM-NOMA with NOMA using ML detection, a significant power gain in the favor of IM-NOMA is clearly noted, which is about 6dB at 10^{-3} BER. This is mainly due to the adoption of IM concept, as activating part of the subcarriers by each user reduces the interference between them. Furthermore, the indexing bits are transmitted with no extra power and can be detected with higher success probability as compared to the complex modulated symbols [42], hence the adoption of IM in NOMA systems improves the error performance. Considering the upper-bound analytical curves of IM-NOMA, the upper bound curve of the the near user (U1) matches the simulation one starting at a transmit power of around 10 dBm while it needs a higher transmit power to match the far one. This is because the far user experiences a lower SNR as compared to the near one at a given transmit power. In Fig. 5, the error performance of IM-NOMA is compared with the Hybrid

IM-NOMA [20] and SM-NOMA [28], under similar configurations as in Fig. 4 with two transmit antennas and one receive antenna ($N_t = 2$, $N_r = 1$) in SM-NOMA. Unlike the Hybrid IM-NOMA, in IM-NOMA the IM concept is applied for all users, hence the inter-user interference (or collision) probability is lower than that when we apply IM on the far user only. This explains the superiority of the near user's (U1) performance in IM-NOMA over the Hybrid IM-NOMA especially at higher transmit power levels. However, the far user (U2) enjoys a similar performance in both schemes. Furthermore, adopting SM in multiple access schemes, as in SM-NOMA, results in involving multiple RF chains [30] which lead to poor power efficiency and higher costs. On the contrary, in IM-NOMA, the IM concept is applied on the subcarriers' indices and a higher spectral and power efficiencies can be achieved that lead to better error performance as clearly seen in the figure.

Unlike the setup in Figs. 4-5 where a single subcarrier is activated per user, in Fig. 6 we set $K = 2$ with $L = N = 3$, $M = 2, 4$ in PD-NOMA and IM-NOMA, respectively, with SIC detection is considered in IM-NOMA. In this setup, a replicated copy of each symbol to be sent to each user is sent over two independent subcarriers which results in a higher

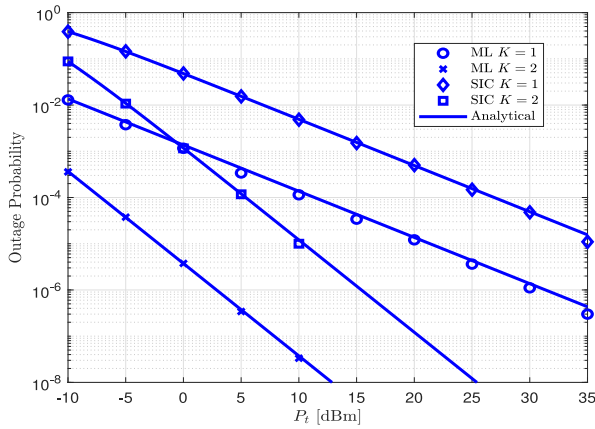


FIGURE 7. The outage probability of the near user, U1, versus P_T with $N = L = M = 2$, $K = 1, 2$, ML and SIC detection.

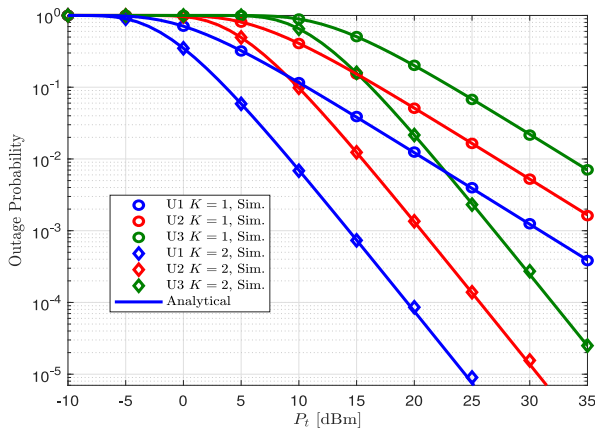


FIGURE 8. The outage probability versus P_T with $N = L = 3$, $M = 2$, $K = 1, 2$ and SIC detection.

transmit diversity gain in IM-NOMA in comparison to that in PD-NOMA as clearly shown in Fig. 6. Furthermore, the curves show that the approximated BER of the N^{th} user in IM-NOMA under SIC, using (17), matches the simulation curve starting at around $P_T = 40$ dBm. It is worth noting here that activating multiple subcarriers per user in IM-NOMA results in coding and transmit diversity gains. The former gain is due to adopting the IM concept and reducing the inter-user interference effect, while the latter is for the reason that we replicate the transmitted symbol over multiple independent subcarriers.

The outage probability for both detection methods is presented in Fig. 7. A setup with $N = L = M = 2$ and $K = 1, 2$ is considered, while only the near user, U1, curves are shown for clarity. The perfect match between the analytical and simulation curves is clear from the figure which validates the analytical derivations of the outage probability for both methods. As expected, the optimal ML detection method outperforms the SIC in terms of outage probability. Furthermore, the diversity gain can be clearly seen from the curves, $d_n = K$, which matches our analytical finding in (29). Similarly, the outage probability is shown in Fig. 8,

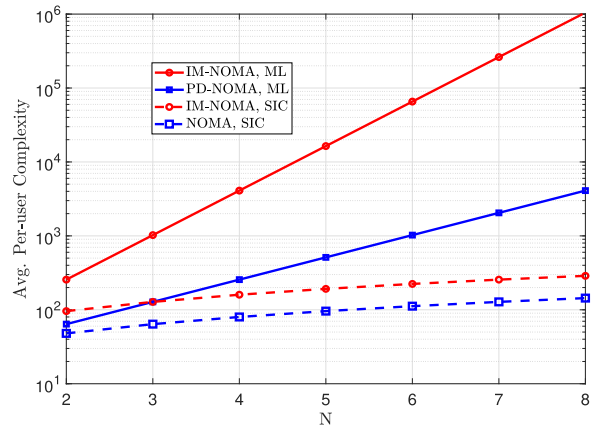


FIGURE 9. The average per-user computational complexity for IM-NOMA and NOMA with $M = L = 2$ and $K = 1$.

with $N = L = 3$ and SIC detection, which verifies the analytical derivations under different parameters and setups.

Finally, the average per-user computational complexity versus the total number of users N for the two schemes PD-NOMA and IM-NOMA based on both ML and SIC is plotted in Fig. 9 with $L = M = 2$ and $K = 1$. As expected, the computational complexity in both schemes increases as the number of users increases. However, due to the inherited drawback of adopting the IM concept, the computational complexity induced by IM-NOMA is higher than that of PD-NOMA. On the other hand, SIC detection can significantly reduce the computational complexity induced by ML detection in both schemes at the cost of performance degradation.

VII. CONCLUSION

In this article, both index modulation and NOMA techniques have been combined to propose a new and efficient downlink multiple access scheme, which is denoted as IM-NOMA. Several performance metrics including error and outage performance of the proposed scheme under maximum likelihood and successive interference cancellation detection techniques have been analyzed. Analytical findings are verified by numerical simulations where it is shown that the proposed scheme enjoys a significantly enhanced performance over classical PD-NOMA. Furthermore, thanks to its superior error performance, more users can be accommodated in IM-NOMA as compared to classical NOMA considering different configurations with an acceptable increase in the computational complexity.

REFERENCES

- [1] S. Chen, H. Xu, D. Liu, B. Hu, and H. Wang, "A vision of IoT: Applications, challenges, and opportunities with China perspective," *IEEE Internet Things J.*, vol. 1, no. 4, pp. 349–359, Aug. 2014.
- [2] H. D. Schotten, M. A. Uusitalo, J. F. Monserrat, and O. Queseth, "5G spectrum: Enabling the future mobile landscape [guest editorial]," *IEEE Commun. Mag.*, vol. 53, no. 7, pp. 16–17, Jul. 2015.
- [3] E. Başar, U. Aygözü, E. Panayirci, and H. V. Poor, "Orthogonal frequency division multiplexing with index modulation," *IEEE Trans. Signal Process.*, vol. 61, no. 22, pp. 5536–5549, Nov. 2013.

- [4] E. Başar, "OFDM with index modulation using coordinate interleaving," *IEEE Wireless Commun. Lett.*, vol. 4, no. 4, pp. 381–384, Aug. 2015.
- [5] M. Nakao and S. Sugiura, "Spectrally efficient frequency division multiplexing with index-modulated non-orthogonal subcarriers," *IEEE Wireless Commun. Lett.*, vol. 8, no. 1, pp. 233–236, Feb. 2019.
- [6] J. Choi and Y. Ko, "TCM for OFDM-IM," *IEEE Wireless Commun. Lett.*, vol. 7, no. 1, pp. 50–53, Feb. 2018.
- [7] M. Wen, Q. Li, E. Basar, and W. Zhang, "Generalized multiple-mode OFDM with index modulation," *IEEE Trans. Wireless Commun.*, vol. 17, no. 10, pp. 6531–6543, Oct. 2018.
- [8] E. Başar, "Multiple-input multiple-output OFDM with index modulation," *IEEE Signal Process. Lett.*, vol. 22, no. 12, pp. 2259–2263, Dec. 2015.
- [9] D. Feng, Q. He, B. Bai, J. Zheng, and M. Liu, "Spatial modulation with multi-dimensional constellations," *IEEE Wireless Commun. Lett.*, vol. 9, no. 1, pp. 99–102, Jan. 2020.
- [10] S. Althunibat and R. Mesleh, "Index modulation for cluster-based wireless sensor networks," *IEEE Trans. Veh. Technol.*, vol. 67, no. 8, pp. 6943–6950, Aug. 2018.
- [11] X. Wu, H. Haas, and P. M. Grant, "Cooperative spatial modulation for cellular networks," *IEEE Trans. Commun.*, vol. 66, no. 8, pp. 3683–3693, Aug. 2018.
- [12] Q. Li, M. Wen, S. Dang, E. Basar, H. V. Poor, and F. Chen, "Opportunistic spectrum sharing based on OFDM with index modulation," *IEEE Trans. Wireless Commun.*, vol. 19, no. 1, pp. 192–204, Jan. 2020.
- [13] J. Zhang, Y. Wang, J. Zhang, and L. Ding, "Polarization shift keying (polarsk): System scheme and performance analysis," *IEEE Trans. Veh. Technol.*, vol. 66, no. 11, pp. 10139–10155, Nov. 2017.
- [14] Y. Cai, Z. Qin, F. Cui, G. Y. Li, and J. A. McCann, "Modulation and multiple access for 5G networks," *IEEE Commun. Surveys Tuts.*, vol. 20, no. 1, pp. 629–646, 1st Quart., 2018.
- [15] L. Dai, B. Wang, Y. Yuan, S. Han, I. Chih-lin, and Z. Wang, "Non-orthogonal multiple access for 5G: solutions, challenges, opportunities, and future research trends," *IEEE Commun. Mag.*, vol. 53, no. 9, pp. 74–81, Sep. 2015.
- [16] S. Timotheou and I. Krikidid, "Fairness for non-orthogonal multiple access in 5G systems," *IEEE Signal Process. Lett.*, vol. 22, no. 10, pp. 1647–1651, Oct. 2015.
- [17] S. Althunibat, R. Mesleh, and T. F. Rahman, "A novel uplink multiple access technique based on index-modulation concept," *IEEE Trans. Commun.*, vol. 67, no. 7, pp. 4848–4855, Jul. 2019.
- [18] S. Althunibat, R. Mesleh, and K. A. Qaraqe, "IM-OFDMA: A novel spectral efficient uplink multiple access based on index modulation," *IEEE Trans. Veh. Technol.*, vol. 68, no. 10, pp. 10315–10319, Oct. 2019.
- [19] S. Althunibat, R. Mesleh, and K. A. Qaraqe, "Quadrature index modulation based multiple access scheme for 5G and beyond," *IEEE Commun. Lett.*, vol. 23, no. 12, pp. 2257–2261, Dec. 2019.
- [20] A. Tusha, S. Dogan, and H. Arslan, "A hybrid downlink NOMA with OFDM and OFDM-IM for beyond 5G wireless networks," *IEEE Signal Process. Lett.*, vol. 27, pp. 491–495, Mar. 2020.
- [21] S. Doğan, A. Tusha, and H. Arslan, "NOMA with index modulation for uplink URLLC through grant-free access," *IEEE J. Sel. Topics Signal Process.*, vol. 13, no. 6, pp. 1249–1257, Oct. 2019.
- [22] J. Li, Q. Li, S. Dang, M. Wen, X.-Q. Jiang, and Y. Peng, "Low-complexity detection for index modulation multiple access," *IEEE Trans. Wireless Commun.*, vol. 9, no. 7, pp. 943–947, Jul. 2020.
- [23] A. Almohamad, M. O. Hasna, S. Althunibat, K. A. Qaraqe, and S. Özyurt, "Low complexity constellation rotation-based SIC detection for IM-NOMA schemes," in *Proc. IEEE 92nd VTC-Fall*, 2020, pp. 1–4.
- [24] T. Wang, F. Yang, and J. Song, "Novel index modulation aided non-orthogonal multiple access for visible light communication," in *Proc. IEEE GLOBECOM Conf.*, 2019, pp. 1–6.
- [25] M. B. Shahab, S. J. Johnson, M. Shirvanimoghaddam, M. Chaffi, E. Basar, and M. Dohler, "Index modulation aided uplink NOMA for massive machine type communications," *IEEE Wireless Commun. Lett.*, vol. 9, no. 12, pp. 2159–2162, Dec. 2020.
- [26] X. Chen, M. Wen, and S. Dang, "On the performance of cooperative OFDM-NOMA system with index modulation," *IEEE Wireless Commun. Lett.*, vol. 9, no. 9, pp. 1346–1350, Sep. 2020.
- [27] R. Y. Mesleh, H. Haas, S. Sinanovic, C. W. Ahn, and S. Yun, "Spatial modulation," *IEEE Trans. Veh. Technol.*, vol. 57, no. 4, pp. 2228–2241, Jul. 2008.
- [28] X. Zhu, Z. Wang, and J. Cao, "NOMA-based spatial modulation," *IEEE Access*, vol. 5, pp. 3790–3800, 2017.
- [29] Q. Li, M. Wen, E. Basar, H. V. Poor, and F. Chen, "Spatial modulation-aided cooperative NOMA: Performance analysis and comparative study," *IEEE J. Sel. Topics Signal Process.*, vol. 13, no. 3, pp. 715–728, Jun. 2019.
- [30] Y. Sun, J. Wang, L. Shi, X. Zhang, and J. Song, "On RF-chain limited spatial modulation aided NOMA: Spectral efficiency analysis," in *Proc. IEEE Globecom Workshops*, 2019, pp. 1–5.
- [31] Y. Chen, L. Wang, Y. Ai, B. Jiao, and L. Hanzo, "Performance analysis of NOMA-SM in vehicle-to-vehicle massive MIMO channels," *IEEE J. Sel. Areas Commun.*, vol. 35, no. 12, pp. 2653–2666, Dec. 2017.
- [32] C. Zhong, X. Hu, X. Chen, D. W. K. Ng, and Z. Zhang, "Spatial modulation assisted multi-antenna non-orthogonal multiple access," *IEEE Wireless Commun.*, vol. 25, no. 2, pp. 61–67, Apr. 2018.
- [33] E. Arslan, A. T. Dogukan, and E. Basar, "Index modulation-based flexible non-orthogonal multiple access," *IEEE Wireless Commun. Lett.*, vol. 9, no. 11, pp. 1942–1946, Nov. 2020.
- [34] Z. Yang, Z. Ding, P. Fan, and G. K. Karagiannidis, "On the performance of non-orthogonal multiple access systems with partial channel information," *IEEE Trans. Commun.*, vol. 64, no. 2, pp. 654–667, Feb. 2016.
- [35] S. Mouchili and S. Hamouda, "Pairing distance resolution and power control for massive connectivity improvement in NOMA systems," *IEEE Trans. Veh. Technol.*, vol. 69, no. 4, pp. 4093–4103, Apr. 2020.
- [36] A. Benjebbovu, A. Li, Y. Saito, Y. Kishiyama, A. Harada, and T. Nakamura, "System-level performance of downlink NOMA for future LTE enhancements," in *Proc. IEEE GLOBECOM Workshops*, 2013, pp. 66–70.
- [37] F. Fang, H. Zhang, J. Cheng, V. C. M. Leung, "Energy-efficient resource allocation for downlink non-orthogonal multiple access network," *IEEE Trans. Commun.*, vol. 64, no. 9, pp. 3722–3732, Sep. 2016.
- [38] H. Jasiulewicz and W. Kordecki, "Convolutions of Erlang and of Pascal distributions with applications to reliability," *Demonstratio Math.*, vol. 36, no. 1, pp. 231–238, 2003.
- [39] A. Almohamad, S. Althunibat, M. O. Hasna, and K. A. Qaraqe, "A downlink index-modulation based nonorthogonal multiple access scheme," in *Proc. IEEE 31st Annu. PIMRC*, 2020, pp. 1–6.
- [40] A. Jeffrey and D. Zwillinger, *Table of Integrals, Series, and Products*. Amsterdam, The Netherlands: Elsevier, 2007.
- [41] I. Thompson, "A note on the real zeros of the incomplete gamma function," *Integral Transforms Spec. Funct.*, vol. 23, no. 6, pp. 445–453, 2012.
- [42] M. Wen, B. Ye, E. Basar, Q. Li, and F. Ji, "Enhanced orthogonal frequency division multiplexing with index modulation," *IEEE Trans. Wireless Commun.*, vol. 16, no. 7, pp. 4786–4801, Jul. 2017.



ABDULLATEEF ALMOHAMAD (Member, IEEE) received the B.S. degree in communication engineering from HIAST, Damascus, Syria, in Fall 2015. He is currently pursuing the master's degree in electrical engineering with Qatar University. He worked as an IP-Backbone Network Engineer with MTN Syria until 2017, before he worked as a Research Assistant with Qatar University in 2018. His research interests falls in the areas of optimization, machine learning, aerial communications and backhauling, index modulation, multiple access schemes, reconfigurable intelligent surfaces, low-power wide area networks, and physical layer security. He is currently volunteered as a TPC Member of IEEE ICC Conference in 2021.



MAZEN O. HASNA (Senior Member, IEEE) received the B.S. degree in electrical engineering from Qatar University, Doha, Qatar, in 1994, the M.Sc. degree in electrical engineering from the University of Southern California, Los Angeles, CA, USA, in 1998, and the Ph.D. degree in electrical engineering from the University of Minnesota Twin Cities, Minneapolis, MN, USA, in 2003. In 2003, he joined the Staff of the Electrical Engineering Department, Qatar University, where he is currently a Professor of Communications. He

has served in several administrative capacities within Qatar University from 2005 to 2017, including the Head of Electrical Engineering Department, the Dean of the College of Engineering, and the VPCAO. His research interests are in the application of digital communication theory to the performance analysis of wireless communication systems. His current specific research interests include aerial networks, D2D enabled communications, physical layer security, FSO/RF hybrid networks, and RIS based communications. He is listed in the 2015 highly cited researchers list of Clarivate Analytics, and has received research grants in the last 10 years worth of more than \$5M, both from industry and government. He Co-Founded and currently serves on the joint management committee of Qatar Mobility Innovation Center, an innovation center promoting using Research and Development to develop and deploy Intelligent Mobility and Smart Cities platforms and technologies. He is an Associate Editor for the IEEE WIRELESS COMMUNICATIONS LETTERS, and an Associate Editor for *Frontiers in Communications and Networks*, and *Frontiers in Space Technologies*. He is a Founding Member of the IEEE Qatar section and has served as its founding VP.



SAUD ALTHUNIBAT (Senior Member, IEEE) is an Associate Professor with the Department of Communications Engineering, Al-Hussein Bin Talal University, Jordan. He is also coordinating the Distinguished Lecturer program in IEEE ComSoc R8. His research interests include non-orthogonal multiple access schemes, index modulation, spatial modulation, cognitive radio, and Internet of Things. He is a member of IEEE ComSoc R8 board.



KHALID QARAQE (Senior Member, IEEE) received the B.S. degree (with Hons.) in electrical engineering from the University of Technology, Bagdad, Iraq, in 1986, the M.S. degree in electrical engineering from the University of Jordan, Amman, Jordan, in 1989, and the Ph.D. degree in electrical engineering from Texas A&M University, College Station, TX, USA, in 1997. From 1989 to 2004, his research interests are in mobile networks, broadband wireless access, cooperative networks, cognitive radio, diversity techniques, index modulation, reconfigurable intelligent surfaces, mmWave, visible light communication, FSO, and telehealth applications.